

## Prediction of post translation modifications at the contact site between *Anaplasma phagocytophilum* and human host during autophagosome induction using a bioinformatic approach

Zarrin Basharat<sup>a,\*</sup>, Sarah Rizwan Qazi<sup>b</sup>, Azra Yasmin<sup>a</sup>, Syed Aoun Ali<sup>c</sup>, Deeba Noreen Baig<sup>c</sup>

<sup>a</sup> Microbiology & Biotechnology Research Lab, Department of Environmental Sciences, Fatima Jinnah Women University, 46000 Rawalpindi, Pakistan

<sup>b</sup> Dr. Panjwani Center for Molecular Medicine and Drug Research, International Center for Chemical and Biological Sciences, University of Karachi, 75270 Karachi, Pakistan

<sup>c</sup> Department of Biological Sciences, Forman Christian College (A Chartered University), 54600 Lahore, Pakistan

### ARTICLE INFO

#### Article history:

Received 15 July 2016

Received in revised form 8 September 2016

Accepted 8 September 2016

Available online xxx

#### Keywords:

*Anaplasma phagocytophilum*

Autophagy

Structure modeling

Molecular docking

Post translational modification

### ABSTRACT

Autophagy is crucial for maintaining physiological homeostasis, but its role in infectious diseases is not yet adequately understood. The binding of *Anaplasma* translocated substrate-1 (ATS1) to the human Beclin1 (BECN1) protein is responsible for the modulation of autophagy pathway. ATS1-BECN1 is a novel type of interaction that facilitates *Anaplasma phagocytophilum* proliferation, leading to intracellular infection via autophagosome induction and segregation from the lysosome. Currently, there is no report of post translational modifications (PTMs) of BECN1 or cross-talk required for ATS-BECN1 complex formation. Prediction/modeling of the cross-talk between phosphorylation and other PTMs (*O*- $\beta$ -glycosylation, sumoylation, methylation and palmitoylation) has been attempted in this study, which might be responsible for regulating function after the interaction of ATS1 with BECN1. PTMs were predicted computationally and mapped onto the interface of the docked ATS1-BECN1 complex. Results show that BECN1 phosphorylation at five residues (Thr91, Ser93, Ser96, Thr141 and Ser234), the interplay with *O*- $\beta$ -glycosylation at three sites (Thr91, Ser93 and Ser96) with ATS1 may be crucial for attachment and, hence, infection. No other PTM site at the BECN1 interface was predicted to associate with ATS1. These findings may have significant clinical implications for understanding the etiology of *Anaplasma* infection and for therapeutic studies.

© 2016 Published by Elsevier Ltd.

### 1. Introduction

*Anaplasma phagocytophilum* is a facultative, intracellular, rickettsial pathogen which infects domestic ruminants and a wide range of mammalian hosts [1,2]. Among them, sheep, cattle and goats are common definitive hosts, while the common zoonotic vector is a tick of the genus *Ixodes* [2]. Varying symptoms are observed in different infected hosts, and it causes granulocytic anaplasmosis in humans through infection of white blood cells and increasing their life span [3]. A type IV secretion system (T4SS) apparatus facilitates transfer of molecules between the bacterium and the host [4]. The bacterium survives by obtaining nutrients in the endosome and by inducing autophagy [5]. Rapamycin induction of autophagy has established that inclusion-targeted autophagosome development supports *A. phagocytophilum* replication [6]. Autophagy induction occurs by bacterial ATS1 binding to the human BECN1, after which the BECN1-Atg14L autophagy initiation pathway is redirected to acquire host nutrients for its own growth [7]. Despite expression of all of the *A. phagocytophilum* T4SS proteins in the leukocytes during anaplasmosis, only T4SS effectors, an ankyrin repeat-rich protein A (AnkA) and ATS1 alter host autophagy mechanism in favour of the bacterial growth [7–10]. On the whole, *A. phagocytophilum* hijacks the host system, suppresses the innate immune response and boosts cholesterol uptake to aid survival [9].

A dual role for ATS1 has been proposed [7]. One portion of ATS1 with a mitochondria-targeting presequence translocates across the outer and inner membranes. The presequence is shed, and the mature ATS1 localizes in the mitochondrial matrix. Mitochondria-localized ATS1 benefits autophagy by delayed apoptosis of host cells. This is accomplished by inhibiting loss of mitochondrial membrane potential. Other portion of ATS1 interacts with the host autophagosome initiation complex (Atg14L-BECN1-Vps34) and stimulates omegasomes in the endoplasmic reticulum. ATS1 is a unique example of a bacterial BECN1 binding protein that takes over the BECN1-Atg14L autophagy initiation pathway, likely to provide nutrients for bacterial growth [7].

The role of phosphorylation is in the regulation of autophagy by AB11 and, consequently, AnkA has been proposed, but information is lacking for this type of modification on BECN1 as well as its impact on ATS1 during autophagy. Phosphorylation has been proposed at the human AB11 protein interface via AB11 tyrosine kinase, which in turn phosphorylates the T4SS effector AnkA at two sites. Other AnkA sites are phosphorylated by Src kinases, which lead to binding of AnkA to the SH2 domain of Shp-1 protein. AnkA protein is then translocated to the nucleus and regulates genes [10].

Phosphorylation is the most important post-translational modification, i.e., the covalent addition of a phosphate group to an amino acid, and impacts functional regulation of proteins [11]. Here, we studied the phosphorylation, other possible PTMs and their cross-talk on BECN1 that might impact on attachment to ATS1 and proliferation. It is difficult and costly to assess this type of cross-talk experimentally, so that

\* Corresponding author.

Email address: zarrin.iiui@gmail.com (Z. Basharat)

an *in silico* approach was employed. A study of phosphorylation and O- $\beta$ -glycosylation interplay using computational tools has previously provided insight into human cellular processes and biological activity as transcription [12], gene expression and virulence potential of human pathogens with implications for therapies in the case of diseases [13]. Artificial neural network (NN) and support vector machine (SVM) based methods are available for predicting various PTMs with substantial precision [14]. This study provides novel insights into the mechanism of bacterial induced autophagy and its modulation of host machinery to cause infection/disease.

## 2. Material and methods

Sequences for human BECN1 (Accession ID: Q14457) and *A. phagocytophilum* ATS1 (Accession ID: Q2GJL5) were retrieved from the Uniprot database.

### 2.1. Sequence analysis

Protein sequences were subjected to an array of analytical methods utilizing various software programs and webservers, in order to understand detailed features, evolution, structure and function during ATS1-BECN1 contact. To assess surface accessibility of BECN1 residues necessary for interaction with ATS1, NetSurfP v1.1 [15] was used. The accuracy of each calculation was determined in the form of a Z-score based on neural networks, which makes efficacy of the prediction reliable. Multiple sequence alignment was carried out using ClustalO (<http://www.ebi.ac.uk/Tools/msa/clustalo/>) to study sequence conservation analysis in two model species. The BECN1 sequence of *Homo sapiens* (human) was compared to those of *Mus musculus* (mouse) and *Rattus norvegicus* (rat) BECN1, with Uniprot accession numbers: O88597 and Q91XJ1, respectively. Secondary structure analyses of BECN1 and ATS1 were conducted using the Polyview server [16]. The conserved domain database (<http://www.ncbi.nlm.nih.gov/Structure/cdd>) of NCBI was explored for studying protein domains.

### 2.2. PTM assessment

Phosphorylation was studied using NetPhos 2.0 [17,18]. This server estimates phosphorylation sites for serine, threonine and tyrosine residues in eukaryotic proteins. Kinases for these phosphorylated sites were determined employing NetPhosK 1.0 [18] and Kinase Phos 2.0 [19] servers that utilize NN and SVM approach. NetPhosK 1.0 includes seventeen kinases (PKA, PKC, PKG, CKII, Cdc2, CaM-II, ATM, DNA PK, Cdk5, p38 MAPK, GSK3, CKI, PKB, RSK, INSR, EGFR and Src), whereas Kinase Phos 2.0 covers 71 kinases. Phosphosites were also mined from the PhosphoELM database [20]. Acetylation was assessed using the NetAcet 1.0 server [21], which reveals substrate residues of N-acetyltransferase A. The prediction algorithm is centered on experimental yeast dataset values, but is known to perform well also for mammalian substrate residues that might be acetylated by NatA orthologs. Methylation modification due to the action of methyl transferases was predicted on arginine and lysine residues by MEMO (<http://www.bioinfo.tsinghua.edu.cn/~tigerchen/memo.html>). Palmitoylation was predicted by CSS-Palm 4.0 (<http://csspalm.biocuckoo.org/online.php>). O-GlcNAcylation was studied using NetOGlyc webserver [22]. The interplay of phosphorylation and O- $\beta$ -GlcNAcylation

was predicted using the YinOYang server [23]. Ubiquitination was predicted using BDM-PUB (<http://bdmpub.biocuckoo.org/prediction.php>), and GPS-SUMO [24] was used for predicting sumoylation at lysine residues.

### 2.3. Structure prediction and molecular docking study

The structure of human BECN1 is available in the Protein Data Bank ([www.rcsb.org](http://www.rcsb.org)). However, to model the protein folds for the region (amino acid residues 1–272) responsible for the interaction with *A. phagocytophilum* ATS1 [7], the complete structure of the BECN1 protein (450 amino acids) was predicted using I-TASSER [25,26]. This server detects templates from the Protein Data Bank by multiple threading method called LOMETS [27], and uses repeated assembly and simulation of template fragments for full-length protein model prediction. Among the predicted models, the best one with the highest C-score and a low root mean square deviation was selected for further analysis, as described previously [28].

The structure of ATS1 has not yet been solved, and has very low homology to existing X-ray and NMR structures in the Protein databank; therefore, it was predicted employing an *ab initio* approach via CABS-fold server (<http://biocomp.chem.uw.edu.pl/CABSfold/index.php>) [29,30]. In addition to root mean square deviation, CABS-fold provides global distance test value for the selection of the best, predicted protein structure (higher values for better structures). These criteria were used for the selection of structures for analysis.

The molecular docking of the BECN1-ATS1 complex was performed using High Ambiguity Driven biomolecular DOCKing (HADDOCK), which takes into account biochemical, biophysical or amalgamated data of both properties [31]. Important residues i-e mid-section of ATS1 (amino acids 90–250) and one-half of human BECN1, including N-terminal (amino acids 1–272) for interaction (determined previously *in vivo* by co-immunoprecipitation, confirmed by reciprocal co-immunoprecipitation [7]), were fed into the HADDOCK server as active site residues. Passive residues were automatically defined around the active site-interacting residues. Other parameters were kept as default.

## 3. Results and discussion

Autophagy, a central macromolecule and organelle degradation process for the maintenance of cell and tissue homeostasis, is vital for cell regulation and allied to numerous human diseases [32]. BECN1 (along with the mammalian class III phosphatidylinositol 3-kinase and Vps34) is an imperative constituent of a complex required for the induction of the autophagosome [33]. It is present during autophagosome formation only and dissociates from the membrane before its maturation [6,34], and is not obligatory for the conventional endosomal/lysosomal pathway [35]. Its interaction/role in invasion and recruitment of the autophagic process for the benefit of the *A. phagocytophilum*, an intracellular rickettsial pathogen of humans, has been explored here using an *in silico* approach.

### 3.1. BECN1 ortholog conservation in human, mouse and rat

Multiple sequence alignment based conservation analysis is of vital importance in model organisms because this can provide an understanding as to whether specific protein and associated biological phe-

nomena are preserved or not. Discoveries made in the model organism provide a basis for insights into the workings of human and other pertinent species. Multiple sequence alignment of BECN1 sequences of human, mouse and rat revealed high protein conservation (Fig. 1). Only 10 residues were different in mouse and 13 in rat as compared with human BECN1, while a difference of 5 residues was seen be-

tween mouse and rat sequences. Deletions at the 7th and 73rd positions were detected in both the rat and mouse sequences. BECN1 was remarkably conserved in sequence among other species as well, showing orthologs in various organisms ranging from yeast to insects, nematodes and amphibians. This information suggests an im-

biolog-

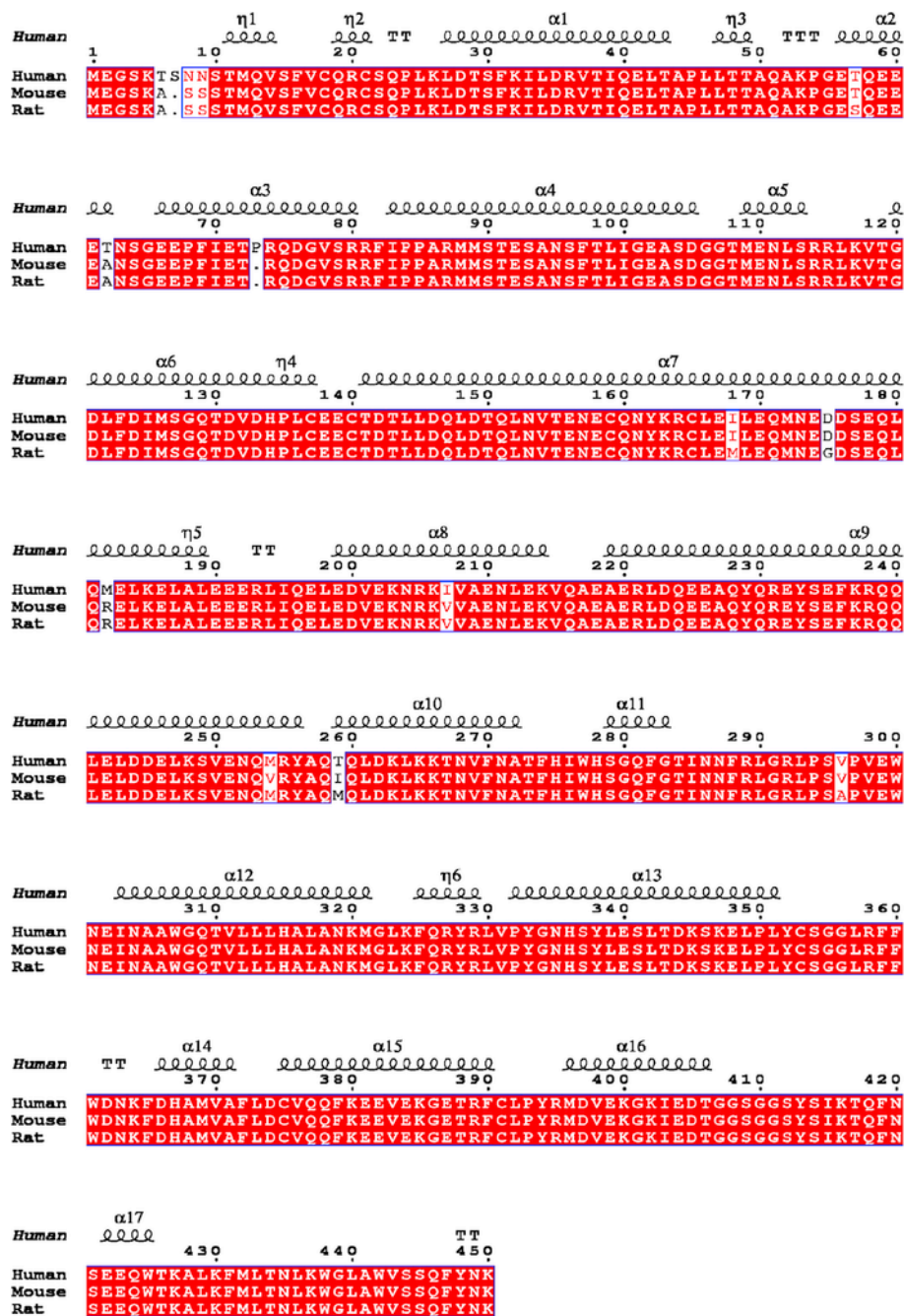


Fig. 1. Alignment of human, mouse and rat BECN1 sequences. Conserved residues are indicated in red whereas dots depict deletions. Secondary structure elements are positioned at the top of the sequence alignment (helices are indicated with squiggles, while turns are shown as Ts). (For interpretation of the references to colour in this figure legend, the reader is referred to the web version of this article.)

ical function of this protein in organismal defence via autophagy (cf. [36]).

3.2. Geometry of BECN1 and ATSI local structure

Hydrogen bonding influences segments of a protein to assume distinct secondary structure. The principal subunit oligomerization motif in BECN1 and ATSI was predicted to be a helix. This category of secondary structure was followed by coil and  $\beta$ -strand/bridge; 299 residues showed a tendency for a helix, 147 for a coil and 4 for a beta-strand/bridge formation in BECN1. In ATSI, 197, 107 and 72 distinct residues had a propensity to form a helix, coil and beta-strand/bridge, respectively. Hydrogen bonds make helical structures particularly stable in both BECN1 and ATSI (Fig. 2).

3.3. Conserved domains in ATSI and BECN1

Three major domains (Fig. 3) are present in BECN1 protein (of 450 amino acids). A Bcl-2 binding (BH3) domain (positions 88–150) [37,38] and a CC domain (residues 144–269) consisting of dimeric alpha helices coiled together [39] and an evolutionarily conserved (EC) domain [37,38]. A heptad repeat (position 177–183), usually labeled ‘abcdefg’ and consisting of residues ‘SEQLQME’ in human and ‘SEQLQRE’ in mouse and rat, is typical of the CC domain. This repeat consists of hxxhxc pattern of amino acids (hydrophobic (h) and charged (c)); position d was occupied by leucine in all organisms studied. The Bcl-2 binding region is conserved among all species investigated. However, 4 residues varied in mouse and 5 in rat. Domains are

a conserved portion of protein that can evolve, function and exist independently of the rest of the protein chain. This depicts a semi-independent feature in a single protein or its sub-units, while domains might evolve independently in orthologs.

A search of the NCBI conserved domain database for BECN1 showed ATP-sensitive microtubule binding component i.e. MT (residues 196–269; E-value:  $8.57 \times 10^{-04}$ ) domain, APG6 domain (residue 135–450; E-value:  $3.98 \times 10^{-163}$ ), chromosome segregation Smc domain (residue 145–266; E-value:  $8.89 \times 10^{-05}$ ) and SMC\_prok\_B domain (residue 145–266; E-value:  $3.96 \times 10^{-04}$ ) likely have a role in cell cycle control, division and chromosome partitioning. Lastly, a type I restriction enzyme hsdR (residues 112–247; E-value:  $9.10 \times 10^{-03}$ ) domain was also mined.

An aromatic finger composed of three hydrophobic residues ‘FFW’ is present between positions 359–361. It arises from core structure and has a deep groove positioned next to it [39]. It is also conserved in human, mouse and rat. In ATSI protein, AF-4 domain (residues 214–320) was detected with an expected threshold of  $4.03 \times 10^{-03}$  (Fig. 4). This domain occurs in AF4 (Proto-oncogene AF4) and FMR2 (Fragile X mental retardation syndrome) nuclear proteins with links to human diseases.

3.4. PTMs regulating BECN1 functioning

Dynamic changes in the protein due to a variety of covalent modifications to amino acid residues relate to functional regulation. PTMs occur at low stoichiometry, and bioinformatics is useful for their analyses. An analysis revealed that a variety of PTMs arise at the BECN1

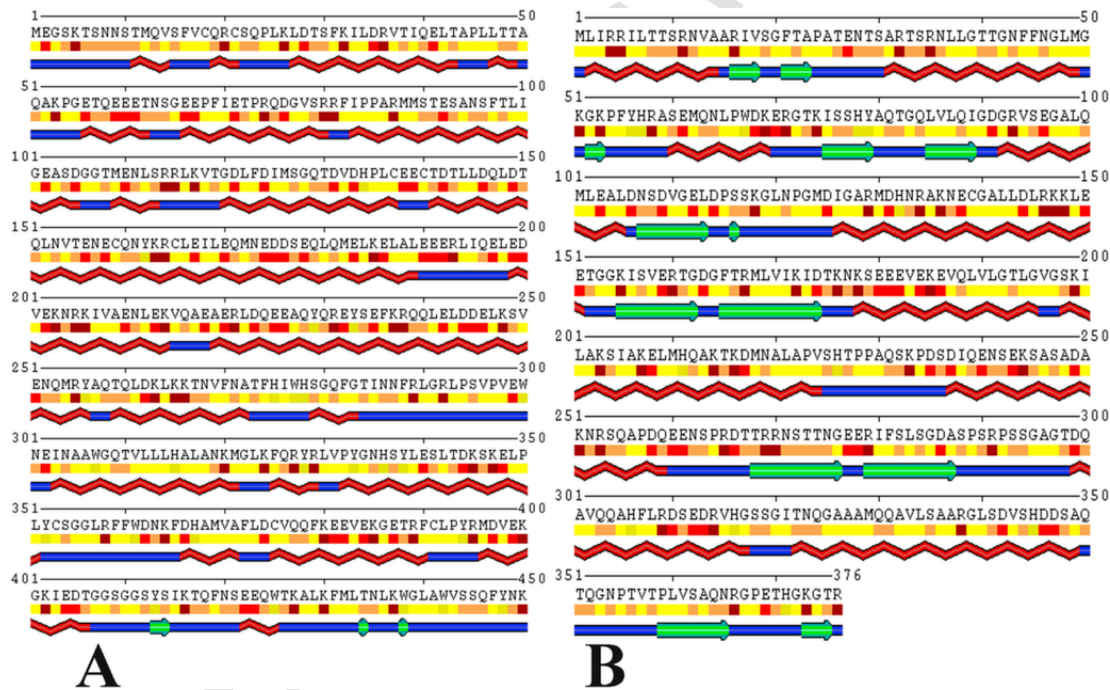
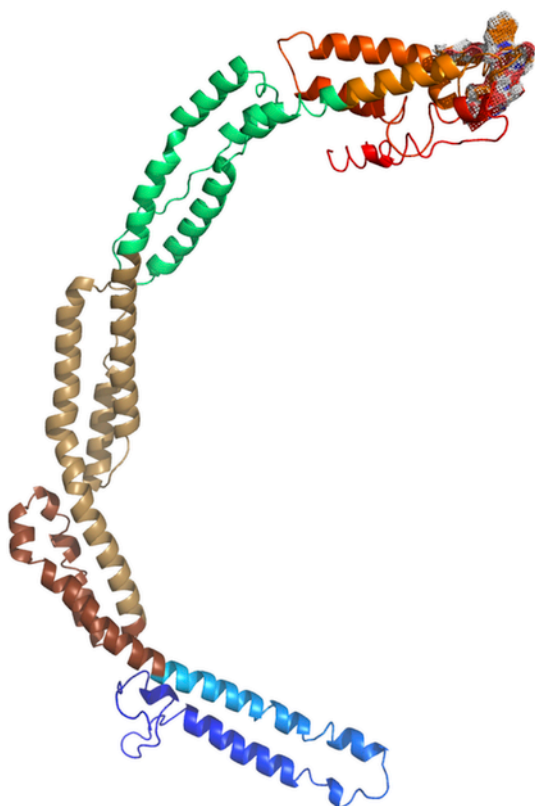
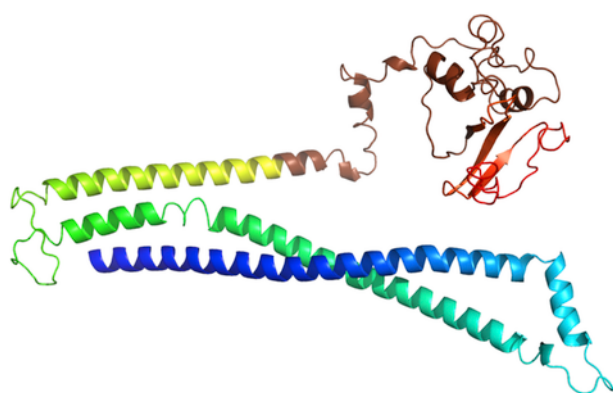


Fig. 2. Secondary structure analysis of (A) Human BECN1 protein and (B) *Anaplasma phagocytophilum* ATSI protein. denotes amino acid residue numeration depicts helices, indicates a  $\beta$ -strand/bridge, and marks a coil. Physico-chemical properties are denoted by, with yellow depicting hydrophobic (A, C, F, G, I, L, M, P and V), followed by amphipathic (H, W and Y), polar (N, Q, S and T), charged residues (negative D, E and positive R and K). (For interpretation of the references to colour in this figure legend, the reader is referred to the web version of this article.)



**Fig. 3.** Three dimensional structure of human BECN1. The Bcl-2 binding domain is shown in brown, CC in gold and ECD in green. The FFW aromatic finger is shown as a mesh. (For interpretation of the references to colour in this figure legend, the reader is referred to the web version of this article.)



**Fig. 4.** The *Anaplasma phagocytophilum* ATS1 protein with N-terminus shown in blue, and the C-terminus depicted in red. The AF-4 domain is shown in brown. (For interpretation of the references to colour in this figure legend, the reader is referred to the web version of this article.)

interface and play an important functional role. A large proportion of residues were predicted to support phosphorylation (69/450) (Table 1). Of 71 amino acid residues displaying phosphorylation, glycosylation and ubiquitination profile (see Table 1), 23 were present in a coiled re-

gion, 3 in beta-bridges, while the rest of them occurred in the helical area. Only one lysine residue at position 402 showed an affinity for methylation, while two cysteines at positions 18 and 21 had an inclination for palmitoylation. None of the amino acid appeared to be acetylated.

Ubiquitination was predicted for 11 lysine residues at positions 5, 26, 53, 117, 237, 266, 320, 324, 345, 416 and 450. A database search revealed two additional lysine sites with a tendency for ubiquitination at positions 430 and 437. Ubiquitination at two sites, i.e. 117 and 437, has also been reported to regulate BECN1 function during autophagy [40]. Sumoylation was predicted for 5 lysine residues at positions 26, 380, 385, 437 and 450. Ubiquitin and Sumo seem to target residue 26 and 450, indicating the possibility of crosstalk between both of these PTMs. Ubiquitination and phosphorylation interplay at position 237 also seems possible for both these PTMs. A considerable number of amino acids showed a tendency for *O*- $\beta$ -GlcNAcylation (20/450), while cross talk of *O*- $\beta$ -GlcNAcylation with phosphorylation was inferred for 11 residues only.

### 3.5. Interaction analysis of BECN1-ATS1

The rapid generation of genetic information via massive sequencing has been associated with the development of computational databases and techniques to extract meaningful information. The development of neural network-based tools, trained on experimental datasets, have the potential to decipher PTMs from sequence data of organisms. It is known that the structure of a mature protein is not reliant solely upon its gene, and PTMs are known to impact variety of protein features, including protein lifecycle, varied enzyme activity and interaction with other proteins [13,41].

Therefore, molecular docking of BECN1-ATS1 was carried out, and PTMs on the interface of BECN1 were identified that might impact interaction. An assessment of PTMs involved in autophagy mediated bacterial take-over of host cell machinery could aid the development of novel methods to thwart bacterial pathogenicity and curb infection/disease.

HADDOCK generated water-refined docked complexes were grouped (51 sets) into 7 clusters. The most reliable cluster with a HADDOCK score of  $428.4 \pm 14.0$ , RMSD value of  $5.8 \pm 1.0$  from the overall lowest-energy structure, Van der Waals energy of  $-131.2 \pm 7.9$ , electrostatic energy  $-662.3 \pm 87.8$ , desolvation energy  $-15.9 \pm 8.7$ , restraints violation energy of  $7078.9 \pm 155.16$ , buried surface area of  $4821.1 \pm 212.3$  and a Z-score of  $-1.6$  was selected for further analysis. The interaction of BECN1 with ATS1 (Fig. 5) showed 22 hydrogen bonds and 70 hydrophobic interactions (Supplementary Table 1). Of these 92 interactions, only five BECN1 residues T91, S93, S96, T141 and S234 associated with ATS1 residues N323, K199, S198, K199 and M168, respectively, showed a tendency for phosphorylation. BECN1 S93, S96 and S234 are proposed to be candidates for PTM-mediated interaction with ATS1, because phosphorylation at these residues has also been reported [40]. An interplay of these phosphorylating sites with *O*- $\beta$ -GlcNAcylation was predicted for three sites (T91, S93 and S96). The BECN1 region critical for attachment to ATS1 (position 1–272) shows six distinct residues in mouse and 8 in rat, but the residues displaying likely phosphorylation and *O*- $\beta$ -GlcNAcylation mediated interaction were conserved among mouse, rat and human. PTM-mediated interaction of

**Table 1**

Study of PTMs of human BECN1 residues. Residues 1–272, which are critical for interaction with AT51, have been underlined. Residues at the interface and carrying PTM interplay potential are shown in bold. Surface accessibility and secondary structure are also indicated. Residue T141, which makes contact with bacterial AT51, was predicted by NetSurfP software to be “buried”, based on sequence information alone. However, three dimensional (3D) structural modeling and docking resolved this issue, and the protein region with this residue appeared to be accessible to enzymes causing PTM as well as for interactions with other proteins.

Residue	Phosphorylation		Kinase phos 2.0	PhosphositePlus database	Glycosylation	YinOYang	Surface accessibility	Secondary structure
	NetPhos 2.0	NetPhosK 1.0			O-GlcNAc			
T6	=	=	<u>GRK, PKB</u>	-	-	Y	E	C
S7	=	=	<u>AKT1, ATM, PKC, Aurora, IKK, PKG, RSK, STK4, CHK1</u>	-	Y	-	E	C
S10	=	=	<u>AKT1, ATM, Aurora, PKG, PLK1, MAPK, RSK, STK4, CHK1</u>	-	-	-	E	C
T11	=	=	<u>GRK, PKB</u>	-	-	Y	E	H
S15	=	<u>cdc2</u>	<u>AKT1, PKA, PKC, PKG, RSK, ATM, STK4, CHK1</u>	-	-	Y	B	C
S22	=	<u>DNAPK</u>	<u>AKT1, ATM, PKC, Aurora, PKG, RSK, CDK, STK4, CHK1</u>	-	-	Y	E	C
T29	=	=	<u>GRK, PKB</u>	-	-	-	E	H
S30	Y	=	<u>AKT1, PKA, PKB, ATM, PKC, IKK, PKG, MAPK, RSK, STK4, CHK1</u>	-	-	-	B	H
T38	=	<u>PKA</u>	<u>GRK, PKB</u>	-	Y	-	E	H
T43	=	=	<u>CRK, PKB</u>	-	Y	-	E	H
T48	=	<u>PKC</u>	<u>GRK, PKB</u>	-	Y	Y	E	H
T49	=	<u>PKC</u>	<u>GRK, PKB</u>	-	Y	-	E	H
T57	Y	<u>CKII</u>	<u>GRK, PKB, CK2, PDK</u>	-	Y	-	E	H
		<u>DNAPK, ATM</u>						
T62		<u>CKII</u>	<u>GRK, PKB, PKC, CDK</u>	-	Y	-	E	H
S64	Y	<u>CKII</u>	<u>AKT1, ATM, Aurora, IKK, PKG, RSK, STK4, CHK1, CK2</u>	-	Y	-	E	C
T72	Y	<u>P32MAPK, Cdk5</u>	<u>GRK, PKB</u>	-	Y	-	E	H
S79	Y	<u>PKC</u>	<u>AKT1, ATM, PKG, RSK, CDK, SDK4, CHK1</u>	-	Y	Y	E	H
S90	Y	<u>RSK, PKG</u>	<u>AKT1, ATM, PKC, PKG, CaM, PLK1, RSK, CDK, STK4, CHK1, CK1</u>	-	Y	-	E	H
T91	=	=	<u>GRK, PKB</u>	-	Y	Y	E	H
S93	=	<u>RSK</u>	<u>AKT1, ATM, IKK, PKG, MAPK, RSK, CDK, STK4, CHK1, CK1</u>	-	Y	-	E	H
S96	=	<u>CKI</u>	<u>AKT1, ATM, IKK, PKG, RSK, STK4, CHK1, CK1</u>	-	Y	-	E	H
T98	=	=	<u>GRK, PKB</u>	-	Y	-	E	H
S104	=	<u>CKI</u>	<u>AKT1, ATM, GSK-3, Aurora, IKK, PKG, PLK1, RSK, CDK, STK4, CHK1</u>	-	Y	-	E	H
T108	=	=	<u>GRK, PKB, CK2, PDK</u>	-	-	-	E	C
S113	=	<u>PKC</u>	<u>AKT1, ATM, GSK-3, PKG, RSK, CDK, STK4, CHK1</u>	-	Y	-	E	H
T119	=	=	<u>GRK, PKB, CK2, PDK</u>	-	Y	Y	B	C
S127	=	=	<u>AKT1, ATM, PKG, MAPK, RSK, STK4, CHK1, CK1, PDK, CK2</u>	-	-	-	E	H
T130	=	<u>CKII</u>	<u>GRK, PKB</u>	-	Y	-	E	H
T141	=	<u>CKII</u>	<u>GRK, PKB</u>	-	-	-	B	H
T143	=	=	<u>GRK, PKB, PKC, CDK</u>	-	-	-	E	H
T150	=	=	<u>GRK, PKB, PKC, CDK</u>	-	-	-	E	H
T155	=	<u>CKII</u>	<u>GRK, PKB, PKC, CDK</u>	-	-	-	B	H
Y162	=	=	<u>Fgr, ALK, PDGFR, BTK, Ret, IGF1R, INSR, IR, EPH, JAK2, TYK2, Fes, ZAP70, FGFR1</u>	-	-	-	B	H
S177	=	<u>CKII</u>	<u>AKT1, GRK, ATM, Aurora, PKG, RSK, CDK, STK4, CHK1, PDK</u>	-	-	-	E	H
Y229	=	=	<u>Fgr, ALK, PDGFR, BTK, Ret, CSK, IGF1R, INSR, EPH, IR, JAK2, TYK2, Fes, ZAP70, FGFR1</u>	P	-	-	B	H
Y233	=	=	<u>FGR, ALK, PDGFR, BTK, Ret, IGF1R, EPH, IR, JAK2, TYK2, Fes, ZAP70, FGFR1</u>	P	-	-	B	H
S234	=	<u>RSK</u>	<u>AKT1, PKB, ATM, PKC, Aurora, PKG, RSK, CDK, STK4, CHK1, CK1</u>	P	-	-	E	H
K237	=	=		P	-	Y	E	H
S249	Y	=	<u>AKT1, PKA, GRK, PKB, ATM, GSK-3, Aurora, IKK, PKG, PLK1, RSK, CDK, STK4, CHK1, CK1</u>	-	-	-	E	H
Y256	=	=	<u>Abl, Fgr, ALK, PDGFR, BTK, Ret, IGF1R, Src, INSR, EPH, IR, JAK2, TYK2, Fes, ZAP70, FGFR1</u>	-	-	-	E	H
T259	Y	<u>PKC</u>	<u>GRK, PKB, PKC, CDK</u>	-	Y	-	E	H
T267	=	=	<u>GRK, PKB, PKC, CDK</u>	-	-	-	E	H
T273	=	=	<u>GRK, PKB</u>	-	-	-	B	C

S279	-	PKA	AKT1, PKA, ATM, PKC, PKG, RSK, STK4, CHK1, PDK	P	-	-	E	H
T284	-	-	GRK, PKB	-	-	-	E	C
S295	-	RSK, PKA	AKT1, PKA, PKB, ATM, GSK-3, Aurora, IKK, PKG, PLK1, RSK, CDK, STK4, CHK1, PAK1	P	-	-	E	C
T310	-	-	GRK, PKB, PKC, CDK, CK2, PDK	-	-	-	B	H

UNCORRECTED PROOF

Table 1 (Continued)

Residue	Phosphorylation			PhosphositePlus database	Glycosylation O-GlcNAc	YinOYang	Surface accessibility	Secondary structure
	NetPhos 2.0	NetPhosK 1.0	Kinase phos 2.0					
Y328	-	-	Fgr, ALK, PDGFR, BTK, IGF1R, EPH, IR, JAK2, TYK2, Fes, ZAP70, FGFR1	-	-	-	B	H
Y333	-	-	ALK, PDGFR, BTK, Ret, IGF1R, EPH, IR, JAK2, TYK2, Fes, ZAP70, FGFR1	-	-	-	E	H
S337	Y	CKII	AKT1, ATM, PKC, IKK, PKG, RSK, STK4, CHK1, CK1, CK2	-	-	-	B	H
Y338	-	-	Fgr, ALK, PDGFR, BTK, Ret, IGF1R, Src, EPH, IR, JAK2, TYK2, Fes, ZAP70, FGFR1	-	-	-	E	H
S341	-	PKC	AKT1, PKB, ATM, GSK-3, PKC, PKG, PLK1, RSK, STK4, CHK1, CK1, CK2	-	-	-	E	H
T343	-	PKC	GRK, PKB	-	-	-	E	H
S346	Y	-	AKT1, PKB, ATM, IKK, PKG, RSK, STK4, CHK1, PDK	-	-	-	E	H
Y352	Y	-	Fgr, ALK, PDGFR, BTK, IGF1R, Src, EPH, IR, JAK2, TYK2, Fes, ZAP70, FGFR1	-	-	-	B	C
S354	-	-	AKT1, PKB, ATM, Aurora, IKK, PKG, MAPK, RSK, CDK, STK4, CHK1, CK1	-	-	-	E	C
T388	-	-	GRK, PKB	-	-	-	E	H
Y394	-	-	Fgr, ALK, PDGFR, BTK, Ret, IGF1R, EPH, IR, JAK2, TYK2, Fes, ZAP70, FGFR1	-	-	-	B	C
T406	-	-	GRK, PKB, PKB, CDK	P	-	-	E	H
S409	-	-	AKT1, ATM, Aurora, PKG, RSK, STK4, CHK1	P	-	-	E	C
S412	-	CK1, PKC, cdc2	AKT1, ATM, Aurora, PKG, RSK, STK4, CHK1, PAK1	-	-	-	E	C
Y413	Y	-	Fgr, ALK, PDGFR, BTK, IGF1R, EGFR, EPH, IR, JAK2, TYK2, Fes, ZAP70, FGFR1	-	-	-	B	E
S414	-	-	AKT1, ATM, IKK, PKG, RSK, STK4, CHK1	-	-	-	B	E
T417	-	-	GRK, PKB, PKC, CDK, CK2, PDK	-	-	-	B	C
S421	-	-	AKT1, PKB, ATM, PKC, PKG, MAPK, RSK, STK4, CHK1, PDK	-	-	-	E	C
T426	-	-	GRK, PKB, CK2, PDK	-	-	-	B	C
K430	-	-		Ub	-	-	B	C
T434	-	PKC	GRK, PKB	-	-	-	B	E
K437	-	-		Ub	-	-	B	C
S444	-	-	AKT1, ATM, PKG, RSK, STK4, CHK1, PDK	-	-	Y	B	C
S445	-	DNAPK, ATM	AKT1, ATM, PKC, PKG, RSK, STK4, CHK1, PDK	-	-	Y	E	C

>0.50 threshold taken as Y (yes) for PTM prediction. Below this threshold, values were taken as insignificant and not considered for depiction in the table or further analysis.

B = Buried residue, E = Exposed residue, P = phosphorylation, Ub = ubiquitination, H = helix, C = coil.

- indicates no information could be inferred. Several of these residues (S14, S90, S93, S96, T108, T119, Y229, Y233, S234, S295 and Y352) are already known to show phosphorylation potential for autophagy related functions [40].

BECN1-ATS1 might be responsible for regulating function following interaction of both proteins.

Residues T91, S93, S96 and T141 are part of the BH3 domain, while S234 lies inside the CC domain. BH3 is an intracellular death-ligand critical for dimerization with other proteins of the Bcl-2 family, crucial for initiating apoptosis and, hence, responsible for their killing activity [42–44], while the CC domain is known to be involved in important biological functions [45,46]. Both domains host residues with potential for phosphorylation-glycosylation interplay in BECN1-ATS1 interaction. These PTMs and their interplay could be vital for pathogen fusion and initiation of apoptosis. Targeting these PTMs, especially kinase mediated phosphorylation (kinases for each residue shown in Table 1), could be important for preventing the cascade of reactions responsible for BECN1-ATS1 fusion and the modulation of autophagy in *A. phagocytophilum*. No other PTM could be predicted for ATS1-interacting residues of BECN1.

Evidence from the literature suggests a critical role of PTMs, especially phosphorylation [47], in regulating the multivalent adapter pro-

tein, i.e. BECN1 during autophagy phenomenon, propagating signals for various other functions and creating binding sites for particular protein segments/binding domains, leading to protein-protein interactions [40,48–50]. Our analysis revealed a cross-link of two important PTMs in regulating bacterial ‘confiscation’ of the host autophagic machinery and its exploitation for instigating infection. Virulence factors of bacteria can exploit human vesicular trafficking, signalling and cytoskeletal pathways for survival by shutting down or evading the defence system [51,52]. Cell function is disturbed, leading to disease. Promising evidence for several bacterial pathogens *Anaplasma phagocytophilum*, *Shigella flexneri*, *Listeria monocytogenes* and *Chlamydia trachomatis* has shown that these microorganisms alter mammalian transcription and chromatin structure, to increase their survival chances and/or overall fitness [52,53]. T4SS of *A. phagocytophilum* links autophagy to bacterial nutrition by binding BECN1, the molecular switchboard in the autophagy-initiating PtdIns3K complex [5]. PTMs at the periphery of BECN1-ATS1 contact are a welcome addition to the blackbox of bacterial molecule-induced autophagy for obtaining nutrients from host



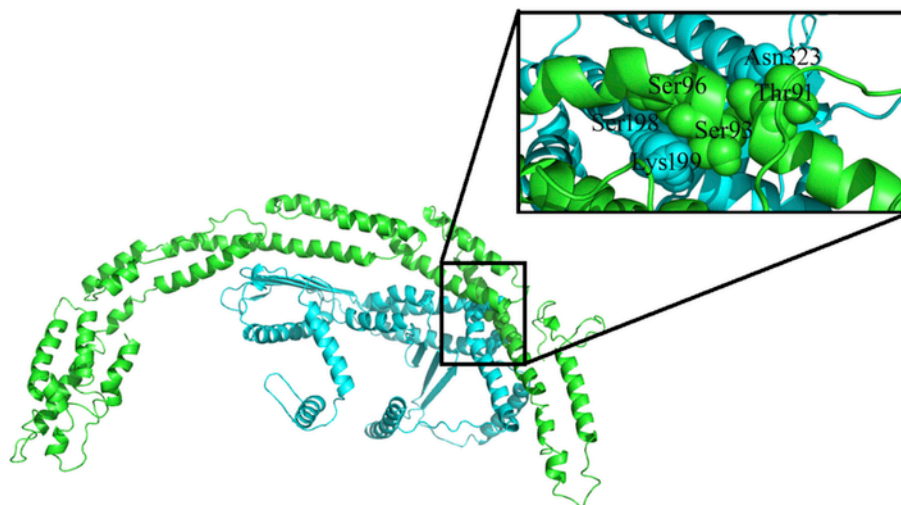


**Fig. 5.** BECN1-ATS1 complex with interaction between the bacterium *Anaplasma phagocytophilum* and the human host cell. BECN1 is shown in green, and ATS1 in blue. Residues proposed to be involved in phosphorylation and *O*- $\beta$ -glycosylation are magnified and labeled. (For interpretation of the references to colour in this figure legend, the reader is referred to the web version of this article.)

cells. The interplay of phosphorylation and *O*- $\beta$ -glycosylation at the BECN1-ATS1 interface might also have implications for drug design against *Anaplasma*. Combinatorial actions of PTMs regulating *Anaplasma* function and infection by other bacteria is also proposed. We recommend further studies of binary PTM switches for controlling protein-protein interactions (especially between host and pathogen), in which one PTM modulates access to or impacts on PTM and, hence, the function(s) of neighbouring sites as well.

#### 4. Conclusion

Our understanding of the molecular phenomena underlying human-microbe interactions and disease has improved in recent years due to the advent of enhanced bioinformatics tools. This study is an attempt to deliver mechanistic insights at sequence, structure and PTM levels for bacterial-induced autophagy that modulates BECN1. ATS1 initiates autophagy by binding BECN1, evading the mTOR starvation signalling pathway. Phosphorylation, glycosylation and multiplicative effects of these PTMs have been focused on BECN1-ATS1 interaction. The functional significance of phosphorylation and glycosylation at the interface of BECN1-ATS1 underlies many unanswered questions about this phenomenon. *A. phagocytophilum* has been previously reported to alter host gene expression through chromatin remodeling and histone modifications to sabotage host pathway and defy innate immunity to establish itself. However, to the best of our knowledge, this is the first computational analysis reporting PTMs in the *A. phagocytophilum* recruitment of human BECN1 and their possible role in the mediation of the autophagic mechanism. This analysis indicates that we are at the threshold of new discoveries using bioinformatics-based approaches for examining PTM mediated molecular interactions that lie at interface of networking protein residues. Spatial, temporal, dynamic, coordinated and/or competitive regulation of PTMs that might influence this interaction need to be further validated, in order to pave way for exciting research, linking PTMs to autophagosome induction by bacteria and intracellular infection via this mechanism.

#### Acknowledgements

The authors are thankful to Alexandra Albakyan for providing literature support. The authors dedicate this manuscript to the revered humanitarian Mr Abdul Sattar Edhi. This research did not receive any specific grant from funding agencies from public, commercial or not-for-profit sectors.

#### Appendix A. Supplementary data

Supplementary data related to this article can be found at <http://dx.doi.org/10.1016/j.mcp.2016.09.002>.

#### Uncited reference

[17].

#### References

- [1] M.S. Severo, K.D. Stephens, M. Kotsyfakis, J.H. Pedra, *Anaplasma phagocytophilum*: deceptively simple or simply deceptive?, *Future Microbiol.* 7 (2012) 719–731.
- [2] S. Stuenkel, G.G. Erik, C. Silaghi, *Anaplasma phagocytophilum* — a widespread multi-host pathogen with highly adaptive strategies, *Front. Cell. Infect. Microbiol.* 3 (2013) 1–33.
- [3] H.C. Lee, M. Kioi, J. Han, R.K. Puri, J.L. Goodman, *Anaplasma phagocytophilum* induced gene expression M in both human neutrophils and HL-60 cells, *Genomics* 92 (2008) 144–151.
- [4] A.B. Russell, R.D. Hood, N.K. Bui, M. LeRoux, W. Vollmer, J.D. Mougous, Type VI secretion delivers bacteriolytic effectors to target cells, *Nature* 475 (2011) 343–347.
- [5] H. Niu, Y. Rikihisa, Ats-1: a novel bacterial molecule that links autophagy to bacterial nutrition, *Autophagy* 9 (2013) 787–788.
- [6] H. Niu, M. Yamaguchi, Y. Rikihisa, Subversion of cellular autophagy by *Anaplasma phagocytophilum*, *Cell. Microbiol.* 10 (2008) 593–605.
- [7] H. Niu, Q. Xiong, A. Yamamoto, M. Hayashi-Nishino, Y. Rikihisa, Autophagosomes induced by a bacterial Beclin1 binding protein facilitate obligatory intracellular infection, *Proc. Natl. Acad. Sci. U. S. A.* 109 (2012) 20800–20807.

- [8] Y. Rikihisa, M. Lin, H. Niu, Microreview: type IV secretion in the obligatory intracellular bacterium *Anaplasma phagocytophilum*, *Cell. Microbiol.* 12 (2010) 1213–1221.
- [9] Y. Rikihisa, Mechanisms of obligatory intracellular infection with *Anaplasma phagocytophilum*, *Clin. Microbiol. Rev.* 24 (2011) 469–489.
- [10] Y. Rikihisa, M. Lin, *Anaplasma phagocytophilum* and *Ehrlichia chaffeensis* type IV secretion and Ank proteins, *Curr. Opin. Microbiol.* 13 (2010) 59–66.
- [11] Y. Huang, B. Xu, X. Zhou, Y. Li, M. Lu, R. Jiang, T. Li, Systematic characterization and prediction of post-translational modification cross-talk, *Mol. Cell. Proteom.* 14 (2015) 761–770.
- [12] A. Kaleem, D.C. Hoessli, I.U. Haq, E. Walker-Nasir, A. Butt, Z. Iqbal, Z. Zamani, A.R. Shakoori, CREB in long-term potentiation in hippocampus: role of post-translational modifications—studies in silico, *J. Cell. Biochem.* 112 (2011) 138–146.
- [13] Z. Basharat, A. Yasmin, In silico assessment of phosphorylation and O- $\beta$ -GlcNAcylation sites in human NPC1 protein critical for Ebola virus entry, *Infect. Genet. Evol.* 34 (2015) 326–338.
- [14] D. Plewczynski, S. Basu, I. Saha, AMS 4.0: consensus prediction of post-translational modifications in protein sequences, *Amino Acids* 43 (2012) 573–582.
- [15] B. Petersen, T.N. Petersen, P. Andersen, M. Nielsen, C. Lundegaard, A generic method for assignment of reliability scores applied to solvent accessibility predictions, *BMC Struct. Biol.* 9 (2009) 1.
- [16] A.A. Porollo, R. Adamczak, J. Meller, POLYVIEW: a flexible visualization tool for structural and functional annotations of proteins, *Bioinformatics* 20 (2004) 2460–2462.
- [17] N. Blom, S. Gammeltoft, S. Brunak, Sequence and structure-based prediction of eukaryotic protein phosphorylation sites, *J. Mol. Biol.* 294 (1999) 1351–1362.
- [18] N. Blom, T. Sicheritz-Pontén, R. Gupta, S. Gammeltoft, S. Brunak, Prediction of post-translational glycosylation and phosphorylation of proteins from the amino acid sequence, *Proteomics* 4 (2004) 1633–1649.
- [19] Y.H. Wong, T.Y. Lee, H.K. Liang, C.M. Huang, T.Y. Wang, Y.H. Yang, C.H. Chu, H.D. Huang, M.T. Ko, J.K. Hwang, KinasePhos 2.0: a web server for identifying protein kinase-specific phosphorylation sites based on sequences and coupling patterns, *Nucleic Acids Res.* 35 (2007) W588–W594.
- [20] H. Dinkel, C. Chica, A. Via, C.M. Gould, L.J. Jensen, T.J. Gibson, F. Diella, Phospho. ELM: a database of phosphorylation sites—update 2011, *Nucleic Acids Res.* (39, 2010). gkq1104.
- [21] L. Kiemer, J.D. Bendtsen, N. Blom, NetAcet: prediction of N-terminal acetylation sites, *Bioinformatics* 21 (2005) 1269–1270.
- [22] C. Steentoft, S.Y. Vakhrushev, H.J. Joshi, Y. Kong, M.B. Vester-Christensen, T. Katrine, B.G. Schjoldager, K. Lavrsen, S. Dabelsteen, N.B. Pedersen, L. Marcos-Silva, Precision mapping of the human O-GalNAc glycoproteome through simple cell technology, *EMBO J.* 32 (2013) 1478–1488.
- [23] R. Gupta, S. Brunak, Prediction of glycosylation across the human proteome and the correlation to protein function. In *Pacific Symposium on Biocomputing*. (2002) 310–322.
- [24] Q. Zhao, Y. Xie, Y. Zheng, S. Jiang, W. Liu, W. Mu, Z. Liu, Y. Zhao, Y. Xue, J. Ren, GPS-SUMO: a tool for the prediction of sumoylation sites and SUMO-interaction motifs, *Nucleic Acids Res.* (42, 2014). gku383.
- [25] Y. Zhang, I-TASSER server for protein 3D structure prediction, *BMC Bioinform.* 9 (2008) 40.
- [26] A. Roy, A. Kucukural, Y. Zhang, I-TASSER: a unified platform for automated protein structure and function prediction, *Nat. Protoc.* 5 (2010) 725–738.
- [27] S. Wu, Y. Zhang, LOMETS: a local meta-threading-server for protein structure prediction, *Nucleic Acids Res.* 35 (2007) 3375–3382.
- [28] Z. Basharat, A. Yasmin, Understanding properties of the master effector of phage shock operon in *Mycobacterium tuberculosis* via bioinformatics approach, *bioRxiv* (2016) 050047.
- [29] A. Kolinski, Protein modeling and structure prediction with a reduced representation, *Acta Biochim. Pol.* 51 (2004).
- [30] M. Jamroz, A. Kolinski, S. Kmiecik, CABS-flex predictions of protein flexibility compared with NMR ensembles, *Bioinformatics* (30, 2014). btu184.
- [31] S.J. De Vries, M. van Dijk, A.M. Bonvin, The HADDOCK web server for data-driven biomolecular docking, *Nat. Protoc.* 5 (2010) 883–897.
- [32] T. Shintani, D.J. Klionsky, Autophagy in health and disease: a double-edged sword, *Science* 306 (2004) 990–995.
- [33] X.H. Liang, S. Jackson, M. Seaman, K. Brown, B. Kempkes, H. Hibshoosh, B. Levine, Induction of autophagy and inhibition of tumorigenesis by beclin 1, *Nature* 402 (1999) 672–676.
- [34] D.J. Klionsky, The molecular machinery of autophagy: unanswered questions, *J. Cell Sci.* 118 (2005) 7–18.
- [35] X. Zeng, J.H. Overmeyer, W.A. Maltese, Functional specificity of the mammalian Beclin-Vps34 PI 3-kinase complex in macroautophagy versus endocytosis and lysosomal enzyme trafficking, *J. Cell Sci.* 119 (2006) 259–270.
- [36] S. Sahni, A.M. Merlot, S. Krishan, P.J. Jansson, D.R. Richardson, Gene of the month: BECN1, *J. Clin. Pathol.* (2014).
- [37] C. He, B. Levine, The beclin 1 interactome, *Curr. Opin. Cell Biol.* 22 (2010) 140–149.
- [38] W. Huang, W. Choi, W. Hu, N. Mi, Q. Guo, M. Ma, M. Liu, Y. Tian, P. Lu, F.L. Wang, H. Deng, Crystal structure and biochemical analyses reveal Beclin 1 as a novel membrane binding protein, *Cell Res.* 22 (2012) 473–489.
- [39] X. Li, L. He, K.H. Che, S.F. Funderburk, L. Pan, N. Pan, M. Zhang, Z. Yue, Y. Zhao, Imperfect interface of Beclin1 coiled-coil domain regulates homodimer and heterodimer formation with Atg14L and UVRAG, *Nat. Commun.* 3 (2012) 662.
- [40] B. Levine, R. Liu, X. Dong, Q. Zhong, Beclin orthologs: integrative hubs of cell signaling, membrane trafficking, and physiology, *Trends Cell Biol.* 25 (2015) 533–544.
- [41] J.W. Kehoe, C.R. Bertozzi, Tyrosine sulfation: a modulator of extracellular protein-protein interactions, *Chem. Biol.* 7 (2000) R57–R61.
- [42] D.T. Chao, S.J. Korsmeyer, BCL-2 family: regulators of cell death, *Ann. Rev. Immunol.* 16 (1998) 395–419.
- [43] T. Chittenden, BH3 domains: intracellular death-ligands critical for initiating apoptosis, *Cancer Cell* 2 (2002) 165–166.
- [44] J.E. Chipuk, T. Moldoveanu, F. Llambi, M.J. Parsons, D.R. Green, The BCL-2 family reunion, *Mol. Cell* 37 (2010) 299–310.
- [45] Y. Weng, Z. Yang, C.D. Weiss, Structure-function studies of the self-assembly domain of the human immunodeficiency virus type 1 transmembrane protein gp41, *J. Virol.* 74 (2000) 5368–5372.
- [46] R.W. Doms, J.P. Moore, HIV-1 Membrane Fusion Targets of Opportunity, *J. Cell. Biol.* 151 (2000) F9–F14.
- [47] Z. Basharat, M. Abdelmonem, S. Ruba, A. Yasmin, NQO1 rs1800566 polymorph is more prone to NOx induced lung injury: endorsing deleterious functionality through informatics approach, *Gene* 591 (2016) 14–20.
- [48] B.T. Seet, I. Dikic, M.M. Zhou, T. Pawson, Reading protein modifications with interaction domains, *Nat. Rev. Mol. Cell Biol.* 7 (2006) 473–483.
- [49] T. Hunter, The age of crosstalk: phosphorylation, ubiquitination, and beyond, *Mol. Cell* 28 (2007) 730–738.
- [50] C. Reidick, F. El Magraoui, H.E. Meyer, H. Stenmark, H.W. Platta, Regulation of the tumor-suppressor function of the class III phosphatidylinositol 3-kinase complex by ubiquitin and SUMO, *Cancers* 7 (2014) 1–29.
- [51] A.P. Bhavsar, J.A. Guttman, B.B. Finlay, Manipulation of host-cell pathways by bacterial pathogens, *Nature* 449 (2007) 827–834.
- [52] E.K. Rennoll-Bankert, D.J. Stephen, Lessons from *Anaplasma phagocytophilum*: chromatin remodeling by bacterial effectors, *Infect. Disord. Drug Targets (Former. Curr. Drug Targets-Infect. Disord.)* 12 (2012) 380–387.
- [53] J.C. Garcia-Garcia, N.C. Barat, S.J. Trembley, J.S. Dumler, Epigenetic silencing of host cell defense genes enhances intracellular survival of the rickettsial pathogen *Anaplasma phagocytophilum*, *PLoS Pathog.* 5 (2009). e1000488.